

# The $N(1520) 3/2^-$ helicity amplitudes from an energy-independent multipole analysis based on new polarization data on photoproduction of neutral pions

J. Hartmann<sup>1</sup>, H. Dutz<sup>2</sup>, A.V. Anisovich<sup>1,3</sup>, D. Bayadilov<sup>1,3</sup>, R. Beck<sup>1</sup>, M. Becker<sup>1</sup>, Y. Beloglazov<sup>3</sup>, A. Berlin<sup>4</sup>, M. Bichow<sup>4</sup>, S. Böse<sup>1</sup>, K.-Th. Brinkmann<sup>1,5</sup>, V. Crede<sup>6</sup>, M. Dieterle<sup>7</sup>, H. Eberhardt<sup>2</sup>, D. Elsner<sup>2</sup>, K. Fornet-Ponse<sup>2</sup>, St. Friedrich<sup>5</sup>, F. Frommberger<sup>2</sup>, Ch. Funke<sup>1</sup>, M. Gottschall<sup>1</sup>, A. Gridnev<sup>3</sup>, M. Grüner<sup>1</sup>, E. Gutz<sup>1,5</sup>, Ch. Hammann<sup>1</sup>, J. Hannappel<sup>2</sup>, V. Hannen<sup>5</sup>, J. Herick<sup>4</sup>, W. Hillert<sup>2</sup>, Ph. Hoffmeister<sup>1</sup>, Ch. Honisch<sup>1</sup>, O. Jahn<sup>2</sup>, T. Jude<sup>2</sup>, A. Käser<sup>7</sup>, D. Kaiser<sup>1</sup>, H. Kalinowsky<sup>1</sup>, F. Kalischewski<sup>1</sup>, P. Klassen<sup>1</sup>, I. Keshelashvili<sup>7</sup>, F. Klein<sup>2</sup>, E. Klempt<sup>1</sup>, K. Koop<sup>1</sup>, B. Krusche<sup>7</sup>, M. Kube<sup>1</sup>, M. Lang<sup>1</sup>, I. Lopatin<sup>3</sup>, K. Makonyi<sup>5</sup>, F. Messi<sup>2</sup>, V. Metag<sup>5</sup>, W. Meyer<sup>4</sup>, J. Müller<sup>1</sup>, M. Nanova<sup>5</sup>, V. Nikonov<sup>1,3</sup>, D. Novinski<sup>3</sup>, R. Novotny<sup>5</sup>, D. Piontek<sup>1</sup>, C. Rosenbaum<sup>1</sup>, B. Roth<sup>4</sup>, G. Reicherz<sup>4</sup>, T. Rostomyan<sup>7</sup>, A. Sarantsev<sup>1,3</sup>, Ch. Schmidt<sup>1</sup>, H. Schmieden<sup>2</sup>, R. Schmitz<sup>1</sup>, T. Seifen<sup>1</sup>, V. Sokhoyan<sup>1</sup>, Ph. Thämer<sup>1</sup>, A. Thiel<sup>1</sup>, U. Thoma<sup>1</sup>, M. Urban<sup>1</sup>, H. van Pee<sup>1</sup>, D. Walther<sup>1</sup>, Ch. Wendel<sup>1</sup>, U. Wiedner<sup>4</sup>, A. Wilson<sup>1,6</sup>, A. Winnebeck<sup>1</sup>, L. Witthauer<sup>7</sup>, and Y. Wunderlich<sup>1</sup>.

(The CBELSA/TAPS Collaboration)

<sup>1</sup>*Helmholtz-Institut für Strahlen- und Kernphysik, Universität Bonn, 53115 Bonn, Germany*

<sup>2</sup>*Physikalisches Institut, Universität Bonn, 53115 Bonn, Germany*

<sup>3</sup>*Petersburg Nuclear Physics Institute, Gatchina, 188300 Russia*

<sup>4</sup>*Institut für Experimentalphysik I, Ruhr-Universität Bochum, 44780 Bochum, Germany*

<sup>5</sup>*II. Physikalisches Institut, Universität Gießen, 35392 Gießen, Germany*

<sup>6</sup>*Department of Physics, Florida State University, Tallahassee, FL 32306, USA*

<sup>7</sup>*Department Physik, Universität Basel, 4056 Basel, Switzerland*

(Dated: July 9, 2014)

New data on the polarization observables  $T$ ,  $P$ , and  $H$  for the reaction  $\gamma p \rightarrow p\pi^0$  are reported. The results are extracted from azimuthal asymmetries when a transversely polarized butanol target and a linearly polarized photon beam are used. The data were taken at the Bonn electron stretcher accelerator ELSA using the CBELSA/TAPS detector. These and earlier data are used to perform a truncated energy-independent partial wave analysis in sliced-energy bins. This energy-independent analysis is compared to the results from energy-dependent partial wave analyses.

It is more than 50 years ago that Chew, Goldberger, Low, and Nambu (CGLN) [1] wrote down the four (complex) amplitudes governing a seemingly simple process in which single pseudoscalar mesons, e.g. pions, are produced off protons or neutrons by photons in the GeV energy range. These four CGLN amplitudes can be expanded into Legendre polynomials and the photoproduction multipoles emerge. The multipoles contain the information on resonances and their properties in a given partial wave. This information can then be extracted in an energy-dependent fit to the multipoles. *At least* eight carefully chosen experiments are required to determine the CGLN amplitudes (up to one arbitrary phase for each bin in energy and angle) in a *complete* experiment [2, 3]. In practice, a significantly larger number of observables need to be known when limitations in statistics and accuracy of experimental data are taken into account [4]. A direct fit to the data with a truncated series of multipoles is certainly more realistic. In the region below the  $2\pi$  threshold,  $S$  and  $P$  waves are sufficient to describe  $\pi^0$  photoproduction, and a measurement of differential cross sections  $d\sigma/d\Omega$  and the photon beam asymmetry  $\Sigma$  is sufficient to determine the contributing multipoles [5, 6]. A minimum of five observables is claimed to be required if the analysis is extended to include higher waves [7, 8]. However, ambiguities may (and will) increase the

number of needed observables. The hope is that photoproduction will overcome the limitations of pion-induced reactions [9] and provide the information to uncover nucleon and  $\Delta$  resonances predicted by quark models (see e.g. [10–12]) - and now in QCD calculations on a lattice [13] - but not found in experiments performed with pion beams. This program requires high-intensity beams of photons up to a few GeV energy with linear and circular polarization, polarized proton and/or neutron targets, and detection of the polarization of the outgoing nucleon. These technical requirements are now all met for a few years, and precise new data including the measurement of double polarization observables start to be published. But still, an unambiguous determination of the four CGLN amplitudes is not yet possible.

In this letter, we present new data on three polarization observables for the reaction

$$\gamma p \rightarrow p\pi^0, \quad (1)$$

thus providing an important next step towards the complete experiment. The observables are the target asymmetry  $T$ , the proton recoil asymmetry  $P$ , and  $H$ , a double polarization observable describing the correlation between beam and target asymmetries. Together with the differential cross section (e.g.[14]) and the data on  $\Sigma$  [15–17],  $G$  [18] and on  $E$  [19] for this reaction, seven observ-

ables have been determined. One might therefore expect that a model-independent construction of photoproduction multipoles for  $S$ ,  $P$ , and  $D$  waves should be possible. The contributions of higher multipoles are expected to be small below  $W = 1600$  MeV; they are approximated by the energy-dependent Bonn-Gatchina (BnGa) fit to a large data base of pion and photo-induced reactions [20].

The energy range for which these seven observables exist covers the  $N(1520)$  resonance with spin and parity  $J^P = 3/2^-$  which decays into  $p\pi^0$  with  $L = 2$ . From the reconstructed  $E_{2-}$  and  $M_{2-}$  multipoles we deduce the  $N(1520) 3/2^-$  photocouplings. It is the first time that data are available which allow for an energy-independent reconstruction of multipoles in the energy range covering the second resonance region ( $N(1520) 3/2^-$  and  $N(1535) 1/2^-$ ).

The experiment was performed at the Bonn ELection Stretcher Accelerator ELSA [21]. Bremsstrahlung photons from a 3.2 GeV electron beam were scattered off a diamond crystal to produce a linearly polarized photon beam [16]. Two orthogonal settings of the polarization plane were used (called  $\parallel$  and  $\perp$ ). The polarization reached its maximum of  $p_\gamma = 65\%$  at 850 MeV and dropped down to 40% at 700 MeV. The polarized photon beam impinged on a butanol ( $C_4H_9OH$ ) target with transversely polarized protons [22]. The mean proton polarization was  $p_T \approx 75\%$ . Data were taken with two opposite settings of the target polarization direction, defined as  $\uparrow$  and  $\downarrow$ .

Neutral pions from the reaction (1) (or from C/O nuclei) were reconstructed from their  $\gamma\gamma$  decay using the CBELSA/TAPS electromagnetic calorimeters. They consist of 1320 CsI(Tl) [23] and 216 forward BaF<sub>2</sub> [24] crystals with a polar angle coverage down to  $1^\circ$  in forward direction. Protons from (1) were detected in the calorimeters as well. In the analysis, events with three distinct calorimeter hits were selected. First they were treated as photon candidates, three  $\gamma\gamma$  invariant masses were formed and a cut on the  $\gamma\gamma$  invariant mass was applied. Then, with the remaining calorimeter hit as the proton candidate, additional cuts to ensure momentum conservation were applied. The resulting event sample contains 1.4 million  $p\pi^0$  events with a background contribution of less than 1% in all energy and angular bins.

The butanol target contained unpolarized C and O nuclei. The dilution factor  $d$  takes into account that photoproduction of  $\pi^0$  off nucleons in C or O nuclei cannot be discriminated completely against reaction (1).  $d$  is a function of  $E_\gamma$  and  $\cos\theta$ , it was determined using data for which the butanol target has been replaced by a carbon foam target inside the cryostat.

In the coordinate frame of the detector we define  $\alpha$  as azimuthal angle of the beam photon polarization plane in the  $\parallel$  setting,  $\beta$  as azimuthal angle of the target polarization vector in the  $\uparrow$  setting, and  $\phi$  as azimuthal angle of the  $\pi^0$ . Then, the differential cross section is modulated

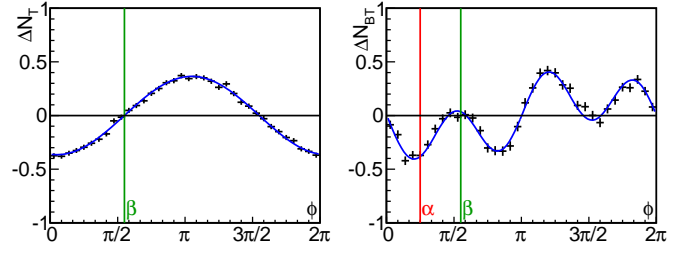


Figure 1: (Color online) Event yield asymmetry as a function of  $\phi$ , left:  $\Delta N(\phi)_T$ , right:  $\Delta N(\phi)_{BT}$ , fitted by the functions given in eqs. (3) and (5), respectively. Both show data from the energy bin  $W = 1.524 - 1.542$  GeV.

according to

$$\frac{d\sigma}{d\Omega} = \left( \frac{d\sigma}{d\Omega} \right)_0 \cdot \{ 1 - p_\gamma \Sigma \cos(2(\alpha - \phi)) + p_T T \sin(\beta - \phi) - p_\gamma p_T P \cos(2(\alpha - \phi)) \sin(\beta - \phi) + p_\gamma p_T H \sin(2(\alpha - \phi)) \cos(\beta - \phi) \}. \quad (2)$$

Since the detector acceptance is identical for all polarization settings, the cross section can be replaced by the normalized yield  $N$ , and the target asymmetry  $T$  is determined from a fit to the azimuthal yield asymmetry:

$$\Delta N(\phi)_T = \frac{1}{d \cdot p_T} \cdot \frac{N_\uparrow - N_\downarrow}{N_\uparrow + N_\downarrow} = T \cdot \sin(\beta - \phi), \quad (3)$$

$$d(E_\gamma, \theta) = \frac{N_{\text{butanol}} - N_{\text{carbon}}}{N_{\text{butanol}}} \quad (4)$$

A typical example for such a fit is shown in Fig. 1, left panel.  $P$  and  $H$  are extracted from data where not only the target polarization is changed but also the photon polarization plane from  $\parallel$  to  $\perp$ , using the equation:

$$\begin{aligned} \Delta N(\phi)_{BT} &= \frac{1}{d \cdot p_\gamma p_T} \cdot \frac{(N_{\perp\uparrow} - N_{\perp\downarrow}) - (N_{\parallel\uparrow} - N_{\parallel\downarrow})}{(N_{\perp\uparrow} + N_{\perp\downarrow}) + (N_{\parallel\uparrow} + N_{\parallel\downarrow})} \\ &= P \sin(\beta - \phi) \cos(2(\alpha - \phi)) - H \cos(\beta - \phi) \sin(2(\alpha - \phi)) \end{aligned} \quad (5)$$

The observables  $P$  and  $H$  are determined by a fit to the  $\Delta N(\phi)_{BT}$  distributions, as shown by the example in Fig. 1, right.

Fig. 2 shows the results for  $T$ ,  $P$ , and  $H$  as functions of the  $\gamma p$  invariant mass  $W$ .  $T$  does not require a polarized photon beam; hence, results are available up to  $W = 2.5$  GeV. The data above  $W = 1.65$  GeV will be shown elsewhere [25]. All three observables are determined simultaneously. The results agree well with previously reported measurements but are more precise and extend the range in both energy and angles. For the double polarization observable  $H$ , no data exist so far below  $W = 1800$  MeV. The agreement with predictions from BnGa2011 [20], MAID [26], and SAID (CM12) [27] is, in general, satisfactory. Larger differences between the different predictions become visible e.g. for  $T$  at forward angles and higher energies. A BnGa refit (solid curve) reproduces the data rather well. The refit includes differential cross sections  $d\sigma/d\Omega$  ( $\chi^2/N_{\text{data}} = 8961/5469$ ) [28], the beam asymmetry  $\Sigma$  (4630/2032) [15–17], and the double polarization variables  $G$  [18] and  $E$  (1197/827) [19].

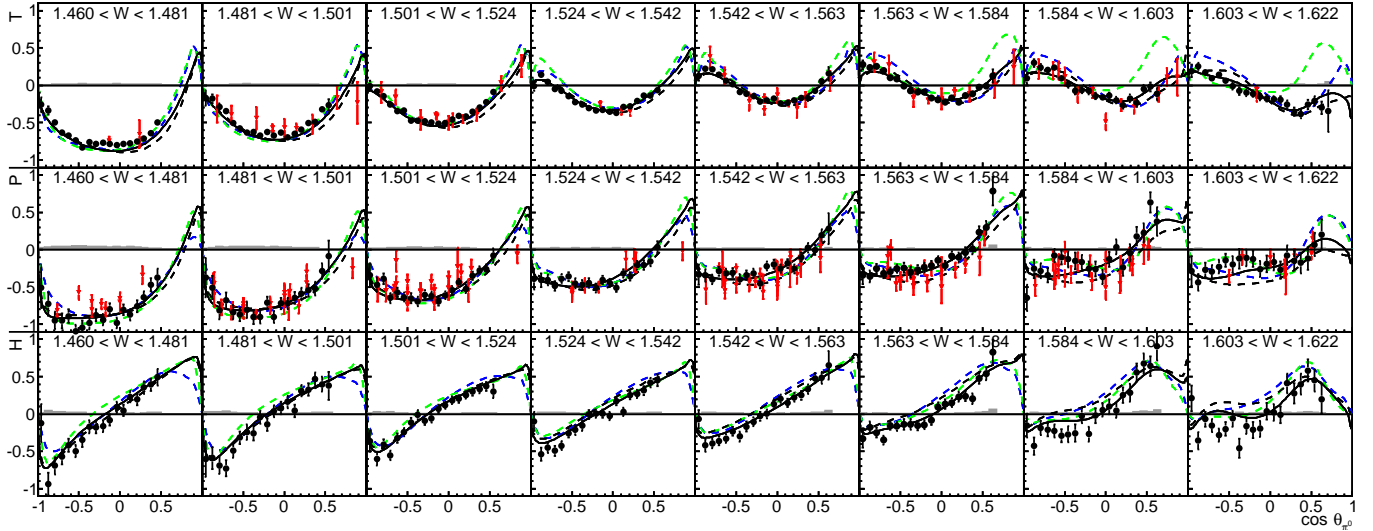


Figure 2: (Color online) The polarization observables  $T$ ,  $P$ , and  $H$  (energy bins in GeV). References to earlier data (gray triangles, (red)) are given in [20], refs. 49-71. The data are compared to predictions (dashed curves) from BnGa2011 (black), MAID (light gray, (green)), and SAID CM12 (dark gray, (blue)). The BnGa refit (BnGa2014) is shown as a black solid line. Similar fits have been performed within the Bonn-Jülich dynamical coupled-channel model [29]. The systematic errors due to the uncertainty in the degrees of proton (2%) and photon (4%) polarizations, in the dilution factor (1%-4%) and the background contamination (0.01 absolute error) are shown as a dark gray band. An additional systematic error on the photon energy reaching from  $\sigma_{E_\gamma}^{\text{sys}} = 6.5$  MeV at the lowest to 5.4 MeV at the highest energy bin plotted is not shown.

The full photoproduction amplitude contains contributions from a series of electric and magnetic multipoles which can be characterized by the orbital angular momentum  $L$  in the decay and the total spin  $J = L \pm 1/2$  of the excited wave. We may expect (and the expectation is supported by partial wave analyses like MAID, SAID and BnGa) that at low energies higher multipoles contribute little to the reaction (1). For an energy-truncated PWA they could hence be neglected. An improved approach is to use instead the according multipoles from a model, e.g. from BnGa2014. Here, we fix all multipoles with  $L \geq 3$  to those from the BnGa energy-dependent partial wave analysis while magnitudes and phases for  $E_{0+}$ ,  $E_{1+}$ ,  $E_{2+}$ ,  $E_{2-}$ ,  $M_{1+}$ ,  $M_{2+}$ , and  $M_{1-}$  are left free. One overall phase remains undetermined, hence we determine the phases relative to the  $M_{2-}$  phase.

The resulting reconstructed multipoles are shown in Fig. 3, except those with magnitudes staying below 1 mfm in the energy region covered here. The small multipoles scatter around small values. Note that a factor 10 in the multipole magnitude corresponds to an intensity ratio of a factor 100.

Most reconstructed multipoles (faint (red) crosses in Fig. 3) are compatible with the energy-dependent analysis, at least at a  $2\sigma$  level even though a few larger discrepancies are observed. But deviations in the magnitude are not accompanied by visible effects in the phase motion; we conclude that these are artifacts of the fit. Indeed, the fit to the data shows not only one isolated minimum; instead other local minima exist which describe angular distributions and polarization observables with similar quality. To choose among these solutions, we applied a

Table I: The  $N(1520) 3/2^-$  helicity amplitudes (in  $\text{GeV}^{-1/2}$ ).

$N(1520) 3/2^-$	this work	CM12 [27]	SN11 [30]	BnGa [20]	PDG [31]
$A_{1/2}$	$-0.022$ $\pm 0.009$	$-0.019$ $\pm 0.002$	$-0.016$ $\pm 0.002$	$-0.022$ $\pm 0.004$	$-0.024$ $\pm 0.009$
$A_{3/2}$	$0.118$ $\pm 0.021$	$0.141$ $\pm 0.002$	$0.156$ $\pm 0.002$	$0.131$ $\pm 0.010$	$0.166$ $\pm 0.005$

penalty function adding to the  $\chi^2$  of the fit the squared difference between the reconstructed multipoles (faint (red) crosses in Fig. 3) and the energy-dependent curve divided by the corresponding statistical error squared. This penalty has hardly any visible impact on the fit to  $P$ ,  $T$  and  $H$ . The resulting reconstructed multipoles – shown as black points with error bars in Fig. 3 – are now fully compatible with the energy-dependent fit.

The reconstructed  $E_{2-}$  and  $M_{2-}$  multipoles receive contributions from both isospins  $I$ ; a separation into  $I = 1/2$  and  $I = 3/2$  contributions is – at present – not possible due to lack of polarization data from the charge-related reaction  $\gamma p \rightarrow n\pi^+$ . But physics helps here: The  $N(1520) 3/2^-$  resonance is far from  $\Delta(1700) 3/2^-$ ; its phase variation in the 1500 MeV region is smooth. We fit the  $E_{2-}$  and  $M_{2-}$  magnitudes (solid crosses in Fig. 3) and their respective phase difference using Breit-Wigner amplitudes together with a background amplitude. The fit returns the  $N(1520) 3/2^-$  helicity couplings (in  $\text{GeV}^{-1/2}$ ), see Table I. The errors comprise the statistical and systematic errors added quadratically. The statistical error for  $A_{1/2}$  is 0.006, and 0.010 for  $A_{3/2}$ . These errors include those contributing to the error band in Fig. 2. The systematic error receives contribution from several sources.

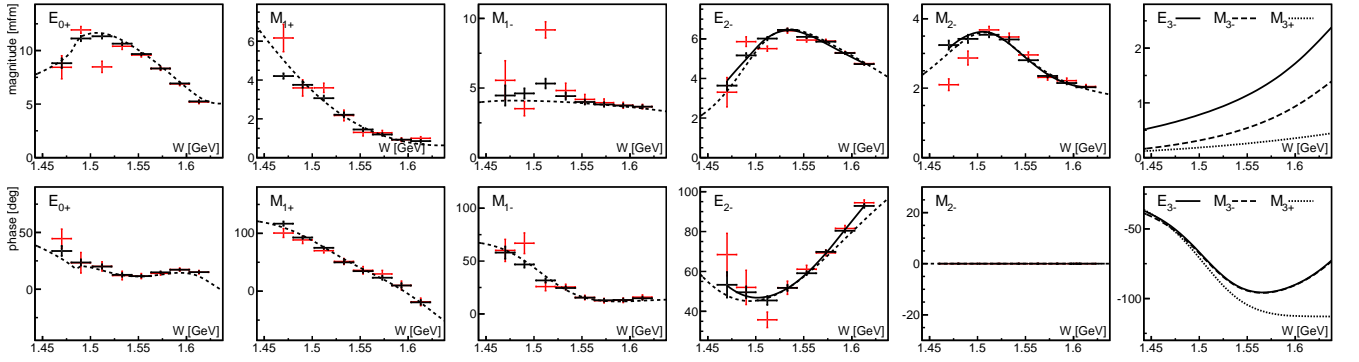


Figure 3: (Color online) Magnitude (upper row) and phase (lower row) of multipoles derived from a fit to data in slices of energy. Grey (red) crosses show the results of an unbiased fit, black crosses represent a fit with a penalty function (see text). The dashed lines show the new energy-dependent Bonn-Gatchina fit (BnGa2014), the solid lines represent a Breit-Wigner plus background fit to the black crosses for  $E_{2-}$  and  $M_{2-}$ . The largest contributions from higher waves (from BnGa2014) are shown as well. The  $E_{3-}$  and  $M_{3-}$  multipoles excite the close-by resonance  $N(1680)5/2^+$ ,  $M_{3+}$  excites  $\Delta(1950)7/2^+$ .

i) The photon energy has an uncertainty of about  $\pm 6$  MeV. We combined data on  $T$ ,  $P$ ,  $H$  with data on  $d\sigma/d\Omega$ ,  $\Sigma$ ,  $E$ ,  $G$  with relative energy shifts of 0,  $\pm 5$ , and  $\pm 10$  MeV, and found no evidence for any systematic shifts but an additional spread of the results. The spread is taken as additional uncertainty. It amounts to 0.005 for  $A_{1/2}$  and to 0.015 for  $A_{3/2}$  (in  $\text{GeV}^{-1/2}$ ). ii) The background amplitude is assumed to be a constant, linear, or quadratic function in  $s$  and/or to be given by the  $\Delta(1700)3/2^-$  amplitude of the energy-dependent fit. The results using different background parameterizations are consistent, their spread is used to define a systematic error, 0.005 for  $A_{1/2}$  and 0.011 for  $A_{3/2}$ . iii) We use a  $N(1520)3/2^- \rightarrow N\pi$  branching ratio of  $0.63 \pm 0.03$ . Its uncertainty is a further systematic error.

In Table I we compare our values for the  $N(1520)3/2^-$  helicity amplitudes with values reported elsewhere. Early results are summarized in PDG 2010 [31]. In particular  $A_{3/2}$  was reported at significantly larger values. The results using the model-independent reconstruction of the amplitudes confirms the results of the BnGa energy-dependent analysis [20] but are at variance with the extremely precise results given by the SAID group [27, 30]. The new result on  $A_{1/2}$  is consistent with earlier determinations. A similar analysis of the  $E_{0+}$  amplitude returns a  $N(1535)1/2^-$  helicity coupling in the range 0.070 to  $0.140 \text{ GeV}^{-1/2}$  depending on the background model.

In summary, we have reported a measurement of three polarization observables,  $P$ ,  $T$ , and  $H$ , for the reaction  $\gamma p \rightarrow p\pi^0$ . These new data represent an important step towards a complete experiment. The data are used to reconstruct multipoles with  $L = 0, 1$  and  $2$ . No evidence for additional structures beyond established resonances is found. The helicity amplitudes of  $N(1520)3/2^-$  are deduced with minimal model assumptions. The result is inconsistent at the level of more than  $2\sigma$  with older (model-dependent) determinations and supports those of the BnGa PWA.

We thank the technical staff of ELSA and the participating institutions for their invaluable contributions to the success of the experiment. We acknowledge support from the *Deutsche Forschungsgemeinschaft* (SFB/TR16) and *Schweizerischer Nationalfonds*.

- 
- [1] G.F. Chew *et al.*, Phys. Rev. **106**, 1345 (1957).
  - [2] I.S. Barker *et al.*, Nucl. Phys. B **95**, 347 (1975).
  - [3] W.-T. Chiang, F. Tabakin, Phys. Rev. **C55**, 2054 (1997).
  - [4] A.M. Satorfi *et al.*, J. Phys. G **38**, 053001 (2011).
  - [5] R. Beck *et al.*, Phys. Rev. Lett. **78**, 606 (1997).
  - [6] G. Blanpied *et al.*, Phys. Rev. Lett. **79**, 4337 (1997).
  - [7] A.S. Omelaenko, Yad. Fiz. **34**, 730 (1981).
  - [8] Y. Wunderlich *et al.*, arXiv:1312.0245 [nucl-th].
  - [9] N. Isgur in Proc. of NSTAR2000, p403, V.D. Burkert, L. Elouadrhiri, J.J. Kelly, R.C. Minehart (eds.), 403.
  - [10] S. Capstick and N. Isgur, Phys. Rev. D **34**, 2809 (1986).
  - [11] U. Löring *et al.*, Eur. Phys. J. A **10**, 395 (2001).
  - [12] E. Santopinto and M.M. Giannini, Phys. Rev. C **86**, 065202 (2012).
  - [13] R.G. Edwards *et al.*, Phys. Rev. D **84**, 074508 (2011).
  - [14] H. van Pee *et al.*, Eur. Phys. J. A **31**, 61 (2007).
  - [15] O. Bartalini *et al.*, Eur. Phys. J. A **26**, 399 (2005).
  - [16] D. Elsner *et al.*, Eur. Phys. J. A **39**, 373 (2009).
  - [17] N. Sparks *et al.*, Phys. Rev. C **81**, 065210 (2010).
  - [18] A. Thiel *et al.*, Phys. Rev. Lett. **109**, 102001 (2012).
  - [19] M. Gottschall *et al.*, Phys. Rev. Lett. **112**, 012003 (2014).
  - [20] A.V. Anisovich *et al.*, Eur. Phys. J. A **48**, 15 (2012).
  - [21] W. Hillert, Eur. Phys. J. **A28S1**, 139 (2006).
  - [22] H. Dutz *et al.*, Phys. Rev. Lett. **93**, 032003 (2004).
  - [23] E. Aker *et al.*, Nucl. Instr. Meth. A **321**, 69 (1992).
  - [24] R. Novotny, IEEE Trans. Nucl. Sci. **NS-38**, 379 (1991).
  - [25] J. Hartmann *et al.*, in preparation.
  - [26] D. Drechsel *et al.*, Nucl. Phys. **A645**, 145 (1999).
  - [27] R. L. Workman *et al.*, Phys. Rev. C **86**, 015202 (2012).
  - [28] W.M. Briscoe *et al.*, gwdaac.phys.gwu.edu/
  - [29] D. Rönchen *et al.*, Eur. Phys. J. A **50**, 101 (2014).
  - [30] R. L. Workman *et al.*, Phys. Rev. C **85**, 025201 (2012).
  - [31] K. Nakamura *et al.*, J. Phys. G **37**, 075021 (2010).